scientific reports

Check for updates

OPEN

Yielding brace system as a next-generation lateral load mechanism for seismic resilient cities

Bush Rc[1]✉, Varsha Rani[2], Anoop I. Shirkol[1]✉, Rohit Vyas[1], Kaushik Gondaliya[3], Pranoy Debnath[4], Ayed E. Alluqmani[5], Yewuhalashet Fissha[6,7], N. Rao Cheepurupalli[8]✉, Refka Ghodhbani[9]✉, Pranjal Mandhaniya[10] & Abdullah Ansari[11,12,13]✉

India's building stock remains highly vulnerable to seismic hazards, with conventional retrofitting strategies often limited in their applicability under varying earthquake intensities. This study investigates the effectiveness of the Yielding Brace System as a novel lateral load–resisting mechanism for improving the seismic resilience of mid-rise reinforced concrete buildings. A six-storey special moment-resisting frame was analysed in bare and Yielding Brace System (YBS)-integrated configurations using a comprehensive multi-analysis framework, including nonlinear static pushover analysis, nonlinear time history analysis, incremental dynamic analysis, and probabilistic fragility assessment. Results demonstrate that the incorporation of YBS significantly reduces inter-storey drift demands by 30–53% and increases normalized base shear capacity from 0.30 in the bare frame to 0.75 in the YBS frame. Ductility improved from 3.20 to 3.98, while residual drift ratios consistently remained below the FEMA P-58/ASCE 41 threshold of 0.5%. Fragility analysis revealed that the bare frame reached a 50% probability of collapse at 5.1 m/s², whereas the YBS-equipped frame required 15 m/s², highlighting a threefold enhancement in collapse safety margin. By reducing collapse probability and ensuring functional recovery after earthquakes, Yielding Brace System advances resilient infrastructure development and aligns with global sustainability objectives under UN SDG 9 (Infrastructure), SDG 11 (Sustainable Cities), and SDG 13 (Climate Action).

Keywords Yielding brace system, Seismic fragility assessment, Incremental dynamic analysis

India is one of the most seismically vulnerable countries in the world, with a long history of devastating earthquakes that have exposed the fragility of its built environment[1]. Major past events, such as the 2001 Bhuj earthquake (magnitude 7.6, approximately 20,023 fatalities), the 1905 Kangra earthquake (magnitude 7.8, approximately 20,000 fatalities), and the 1993 Latur earthquake (magnitude 6.2, approximately 9,748 fatalities)[2], highlight the catastrophic impact of seismic disasters on life, property, and infrastructure. A critical lesson repeatedly demonstrated is that earthquakes themselves do not kill people; rather, weak and poorly designed buildings are responsible for large-scale collapses and fatalities[3,4]. Outdated and structurally deficient buildings fail to withstand the extreme lateral and vertical forces generated during seismic events, leading to cracks, foundation failures, and widespread destruction[5].

[1]Department of Civil Engineering, Malaviya National Institute of Technology Jaipur, Jaipur 302017, India. [2]Government Polytechnic Purnea, Purnia, Bihar, India. [3]Department of Civil (Structural Engineering), School of Engineering and Technology, GTU, Ahmedabad, India. [4]Department of Civil Engineering, Indian Institute of Technology Bombay, Mumbai 400076, Maharashtra, India. [5]Department of Civil Engineering, Faculty of Engineering, Islamic University of Madinah, Al-Madinah Al-Munawarah, Saudi Arabia. [6]Department of Electrical and Computer Engineering, National Institute of Technology, Asahikawa College, 2-2-1-6 Syunkodai, Asahikawa city Hokkaido 071-8142, Japan. [7]Department of Mining Engineering, Aksum University, Aksum, Tigray 7080, Ethiopia. [8]Department of Mineral Processing and Metallurgical Engineering, Faculty of Mines, Aksum University, Axum, Ethiopia. [9]Center for Scientific Research and Entrepreneurship, Northern Border University, Arar 73213, Saudi Arabia. [10]Department of Mechanical and Industrial Engineering, Norwegian University of Science and Technology Trondheim, Trondheim, Norway. [11]Earthquake Monitoring Center, Sultan Qaboos University, Muscat, Al Khoudh PC: 123, Oman. [12]Department of Civil Engineering, Inha University, Incheon, Republic of Korea. [13]Faculty of Civil Engineering, Istanbul Technical University, ITU Ayazaga Campus, Istanbul, Maslak 34469, Turkey. ✉email: 2021rce9516@mnit.ac.in; 2020RCE9515@mnit.ac.in; anoop.ce@mnit.ac.in; nraocheepurupalli@gmail.com; Refka.Ghodhbani@nbu.edu.sa; a.ansari@squ.edu.om

The Global Earthquake Model (GEM) open-source seismic risk assessment (Fig. 1) provides a comprehensive profile of India's earthquake hazard[6], exposure, and vulnerability. From a hazard perspective, the Himalayan belt, northeast India, and parts of Gujarat and Bihar exhibit the highest seismic hazard[7,8], with peak ground accelerations exceeding 0.3–0.5 g under a 475-year return period event[6]. Central and southern India remain comparatively less hazardous, though not entirely exempt from risk. Exposure mapping indicates that economically significant regions such as Delhi, Mumbai, Gujarat, and Kolkata possess very high concentrations of built assets, thereby amplifying the potential financial losses during a major seismic event. The average annual loss (AAL) for India is estimated at 1.34 billion USD, with residential buildings contributing the highest share (approximately 1.11 billion USD), followed by commercial (approximately 0.19 billion USD) and industrial (approximately 0.03 billion USD) sectors. In terms of average annual loss ratio (AALR), which measures expected annual losses relative to the replacement cost, the national figure stands at 0.449%, but regional variations are pronounced. North-eastern states and the Himalayan region show the highest AALR values (2.8–5.1% and above), indicating disproportionate losses relative to local building stock. Loss-by-region statistics further emphasize the vulnerability of populous states such as Uttar Pradesh, Bihar, Punjab, Assam, and Jammu & Kashmir, each facing hundreds of millions of dollars in potential annualized seismic losses. The building taxonomy underscores India's structural fragility, as a large proportion of the building stock consists of confined masonry (33%) and concrete structures (25%), alongside unreinforced masonry, adobe/earth, and other traditional systems that lack adequate seismic resistance. Such construction classes are particularly prone to collapse under lateral shaking, thereby elevating casualty and economic loss risks. Loss curves generated under the GEM framework project that rare but extreme earthquakes with return periods of 500 to 1,000 years could trigger economic losses between 44 and 60 billion USD, underscoring the urgent need for robust risk mitigation strategies[6].

Earthquake-resistant structural design requires more than material strength; it demands a comprehensive understanding of how seismic forces interact with structural systems. Key parameters such as base shear, resonance, damping efficiency, and torsional stability govern whether a structure can withstand seismic excitations or progress toward collapse[9] Although seismic codes have significantly advanced structural safety[7,8,10], a vast proportion of existing buildings remain critically vulnerable due to outdated construction practices[11], weak lateral bracing, and inadequate energy dissipation.

In recent years, advancements in passive energy dissipation devices have introduced several innovative solutions to overcome these limitations. Among them, the Rotational Steel Rod Damper (RSRD) has emerged as a promising metallic device designed to enhance seismic resilience through plastic rotation of low-yield-point steel rods. Zhou et al. (2024)[12] demonstrated its stable hysteretic performance ($\zeta > 0.47$) and improved fatigue

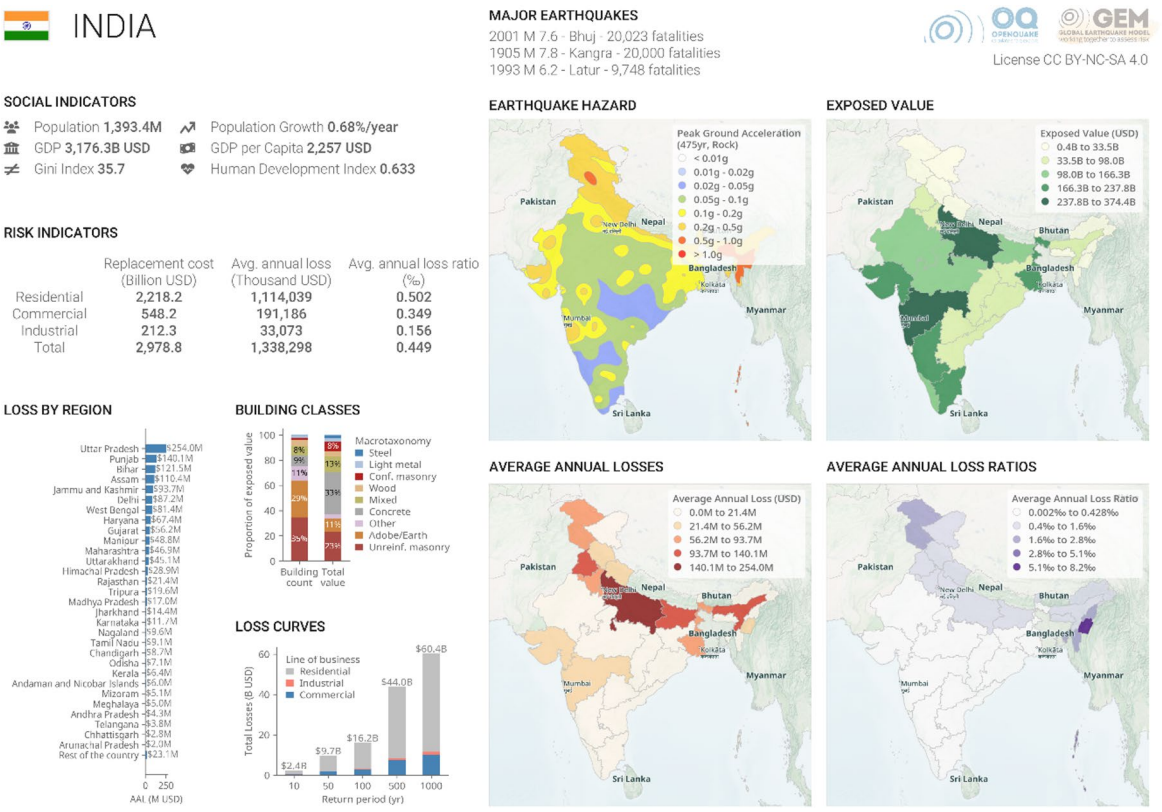

Fig. 1. Seismic hazard, exposure, and risk indicators for India based on the Global Earthquake Model (GEM) open-source assessment. [adapted from GEM Foundation, India Seismic Risk Profiles, 2023, CC BY-NC-SA 4.0 (https://www.globalquakemodel.org/product/seismic-risk-profiles)][6].

resistance achieved through arc-shaped weakening of the rods. Lie et al. (2024)[13] applied the RSRD in a hybrid retrofit configuration combining Damping Masonry Infill Walls (DMIWs), achieving up to 38% reduction in floor acceleration and improved drift uniformity. Later, Lie et al. (2025)[14] extended its application as a dissipative connector in rocking steel core systems, where hourglass-shaped rods enhanced low-cycle fatigue resistance. Overall, RSRDs have shown consistent energy dissipation ($\zeta \approx 0.5$) and effective drift control, demonstrating their versatility and reliability across both RC and steel structural systems.

Conventional solutions, including tuned mass dampers, viscous dampers, and buckling restrained braces (BRBs)[15–17], have improved seismic resilience but often perform optimally only within narrow force thresholds, limiting their applicability in real-world conditions where earthquake intensities vary unpredictably. Despite their widespread use, BRBs exhibit several practical and performance limitations that restrict their efficiency under severe or repeated earthquakes. The steel core of a BRB is fully enclosed within its restraining casing, making post-earthquake inspection and replacement difficult, while hidden yielding often prevents accurate damage assessment. Furthermore, BRBs lack self-centering capability, resulting in permanent residual drifts and increased repair costs after strong ground motions. Studies by Bobadilla et al. (2025)[18] and Hoveidae (2018)[19] have also shown that BRBs undergo cumulative ductility degradation and low-cycle fatigue damage under repeated cyclic loading, reducing their long-term energy dissipation capacity.

In this context, the Yielding Brace System (YBS) represents a transformative solution as shown in Fig. 2[22]. Unlike BRBs or conventional damping devices, YBS offers superior seismic energy dissipation across a broad range of loading conditions, ensuring stability under both moderate and extreme earthquakes[20]. Its high ductility, capacity to absorb cyclic energy without premature degradation, and adaptability for both new construction and retrofitting make it a cost-effective and practical alternative for modern seismic design. YBS not only enhances lateral load resistance but also addresses soft-story vulnerabilities without necessitating major reconstruction, making it particularly suitable for dense urban environments. Despite its remarkable potential, YBS remains underexplored in seismic engineering research, creating a significant knowledge gap.

To address this, the present study investigates the seismic performance of a six-storey reinforced concrete (RC) building with and without YBS integration through a multi-analysis framework. Nonlinear static pushover analysis (NSPA) is employed to assess global capacity, performance points, and comparative lateral strength. Nonlinear time history analysis (NLTHA) captures realistic dynamic responses, including inertia effects, cyclic degradation, and higher mode contributions under recorded earthquake excitations. Incremental dynamic analysis (IDA) is utilized to establish intensity–response relationships, evaluate collapse margin ratios, and quantify safety margins across seismic intensities. Finally, seismic fragility assessment provides probabilistic estimates of exceeding predefined damage states at varying hazard levels.

Methodology

In this study, the seismic performance was evaluated considering a target drift limit of 2%. Table.

Spectral modal and pushover analyses were carried out to estimate storey shear forces and drift demands, which were then compared against code-specified limits to assess the structural response. The force–displacement capacity, size selection, and placement procedure for the YBS were adapted from previous research studies[22]. The percentage of storey shear to be resisted by the secondary system was defined, and the number and location of YBS units on each floor were determined to ensure a torsion-free configuration. The design strength of each YBS unit was calculated, and its nonlinear hysteretic behaviour was modelled in ETABS software[23] using the Bouc–Wen model[24], incorporating stiffness, weight, post-yield stiffness ratio, and yielding exponent values calibrated from experimental data. Figure 3 presents the YBS design and Hollow Structural Section (HSS) selection

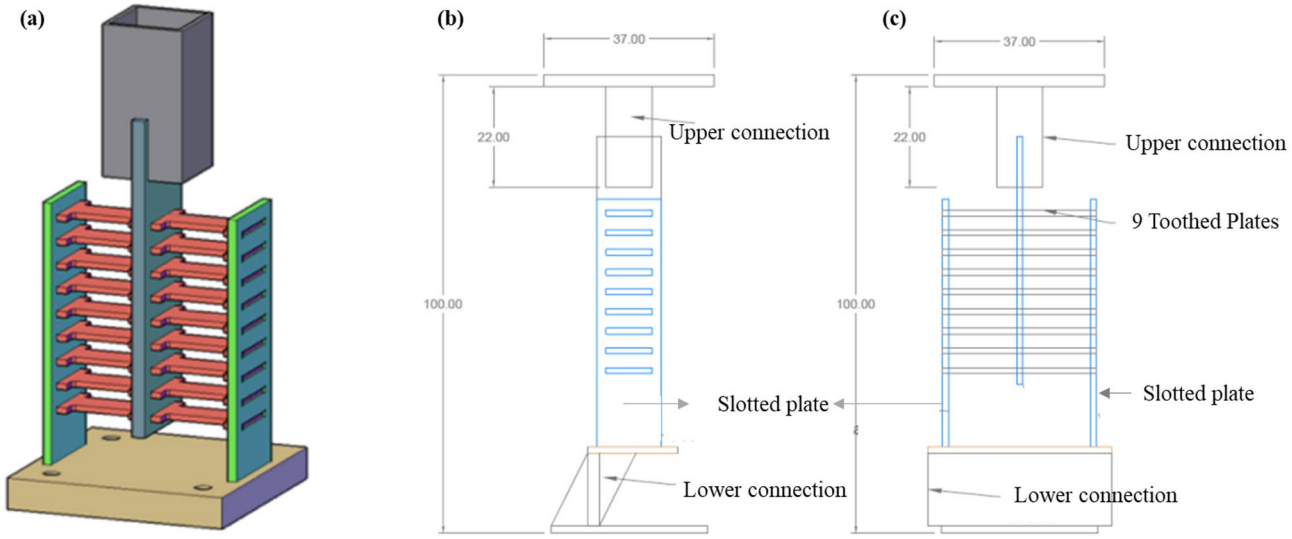

Fig. 2. Proposed YBS Details with Dimensions[21].

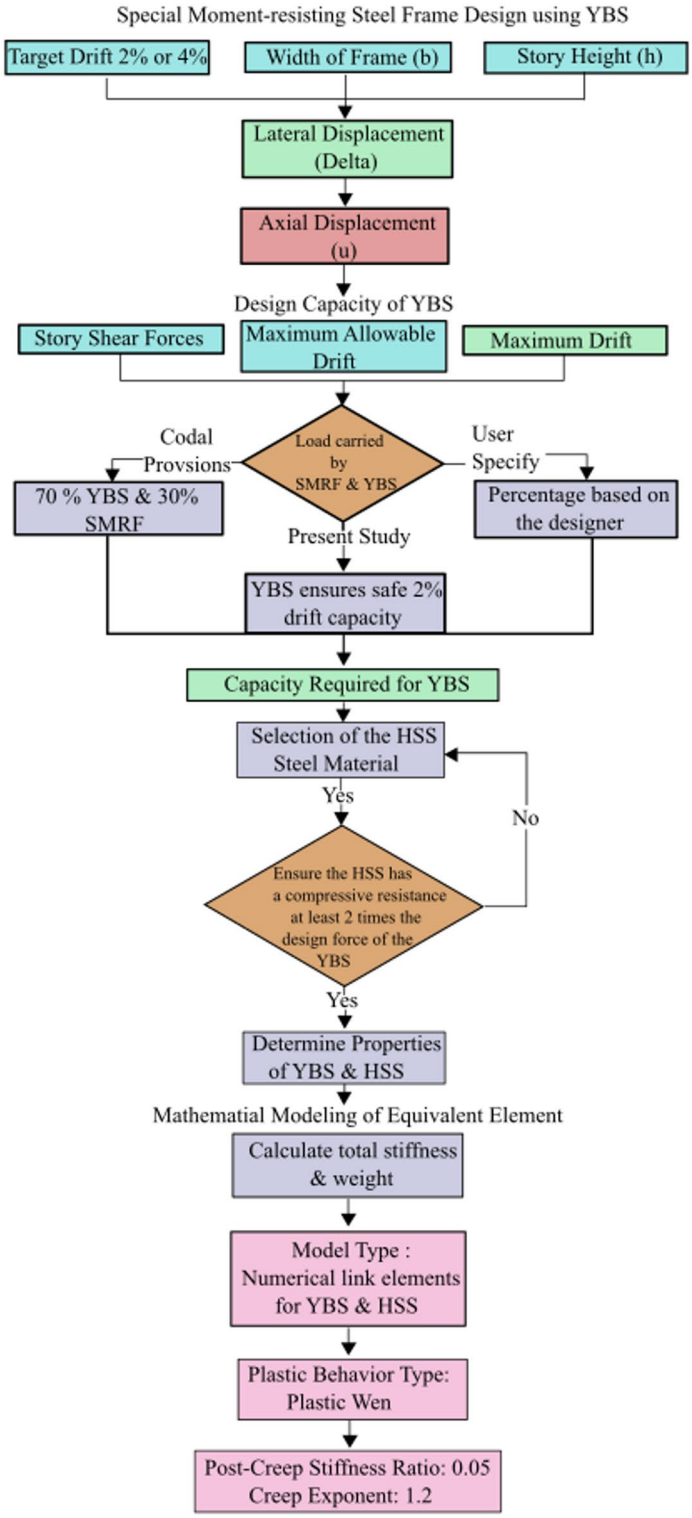

Fig. 3. Workflow for Yielding Brace System (YBS) design and Hollow Structural Section (HSS) selection.

workflow, outlining the step-by-step process for determining the required stiffness, strength, and weight of the system.

Nonlinear modelling was carried out using the fibre modelling approach to accurately capture material stress–strain behaviour and inelastic response[25]. The stress–strain relationship for concrete was defined using the Mander et al. (1988) model[26], while the Park model was adopted for steel. Degrading hysteretic behaviour was considered for both materials. Fibre cross-sections were divided into 24 segments, with appropriate stress–strain values assigned to each segment[22]. The fibre hinge length was taken as half of the maximum section

dimension, with P-M2-M3 hinges used for columns and M3 hinges for beams[25]. The plastic hinge length was determined following the approach of Priestley et al. (1996)[27], with flexural hinges assumed to form at a distance of half the hinge length from the member ends.

Before the main analyses, a validation study was carried out to verify the numerical modelling of YBS. Figure 4 illustrates the validation process, which compares hysteretic behaviour from experimental and analytical studies. The experimental results were obtained from Dampo Systems (Mexico)[21] using the loading protocol specified in ASCE/SEI 41-17[28], while the analytical validation was performed in ETABS Software[23] using the same recommended loading protocol. The close agreement in energy dissipation, stiffness degradation, and ductility confirmed the accuracy of the adopted modelling approach.

Seismic evaluation was conducted using two analytical approaches: NSPA and IDA. In NSPA, the pushover curve was converted to a capacity spectrum to obtain spectral displacement values, which were then fitted to statistical distributions to establish damage state thresholds and estimate uncertainties. Figure 5 outlines the process for developing fragility curves, starting from model setup and ground motion selection to statistical fitting for probability of exceedance at defined damage states. The results from both NSPA and IDA were used to define limit states (slight, moderate, severe, and collapse) and develop fragility curves representing the probability of collapse at various seismic intensities. This methodology enabled a comparative assessment of the structural performance of the RC frame with and without YBS, quantifying improvements in ductility, stiffness, energy dissipation capacity, and reduction in collapse probability.

Modeling of RC frame with YBS

To assess the effectiveness of the YBS, a six-story, plan-symmetric RC frame was developed as the reference model as shown in Fig. 6. The building configuration represents a typical mid-rise apartment commonly constructed in India. The structure is assumed to be located in seismic Zone V, the region of highest seismicity, with an effective peak ground acceleration (EPGA) of 0.36 g, and is considered to rest on soft soil. The frame was designed with a bay span of 4 m (Fig. 6a) and a story height of 3 m. Floor finish and live loads were taken as 1 kN/m² and 3 kN/m², respectively, while 150 mm thick RC slabs were modeled as rigid diaphragms. Columns were assumed to have fixed base conditions. Dead loads included the self-weight of beams, columns, slabs, and walls in accordance with IS 875: Part 1 (BIS 1987a)[28], and live loads were considered as per IS 875: Part 2 (BIS 1987b)[29]. The RC frame was designed as a special moment-resisting frame (SMRF) with a response reduction factor (R) of 5, and ductile detailing provisions were followed as per IS 13,920 (BIS 2016b)[30]. Structural design used M25 grade concrete and Fe500 reinforcement steel. Seismic demands were obtained using the response spectrum method. Effective stiffness values of 0.35Igross for beams and 0.70Igross for columns were adopted, along with a rigid zone factor of 0.5 at beam–column joints to capture partial fixity and realistic joint stiffness. Linear and nonlinear analyses were carried out using ETABS (CSI 2020)[23], following IS 456 (BIS 2000)[31], IS 1893 (BIS 2016a)[7], and IS 13,920 (BIS 2016b)[30]. Load combinations were defined according to IS 1893 (BIS 2016a)[7]. Member sizes were finalized based on demand–capacity checks while maintaining the strong-column weak-beam principle. The YBS was placed at the center of the building frame to enhance its seismic capacity and overall performance as illustrated in Fig. 6(b).

The size, section, and stiffness of the YBS were obtained from the displacement-controlled pushover analysis carried out up to the 2% target drift level, which corresponds to the permissible drift for RC buildings without masonry infill as specified in ASCE 7 (ASCE/SEI 2016)[10]. The results at this drift level were used as the basis for defining the YBS properties in accordance with the strong column–weak beam design philosophy. The adopted YBS configuration for the six-story frame is presented in Table 1.

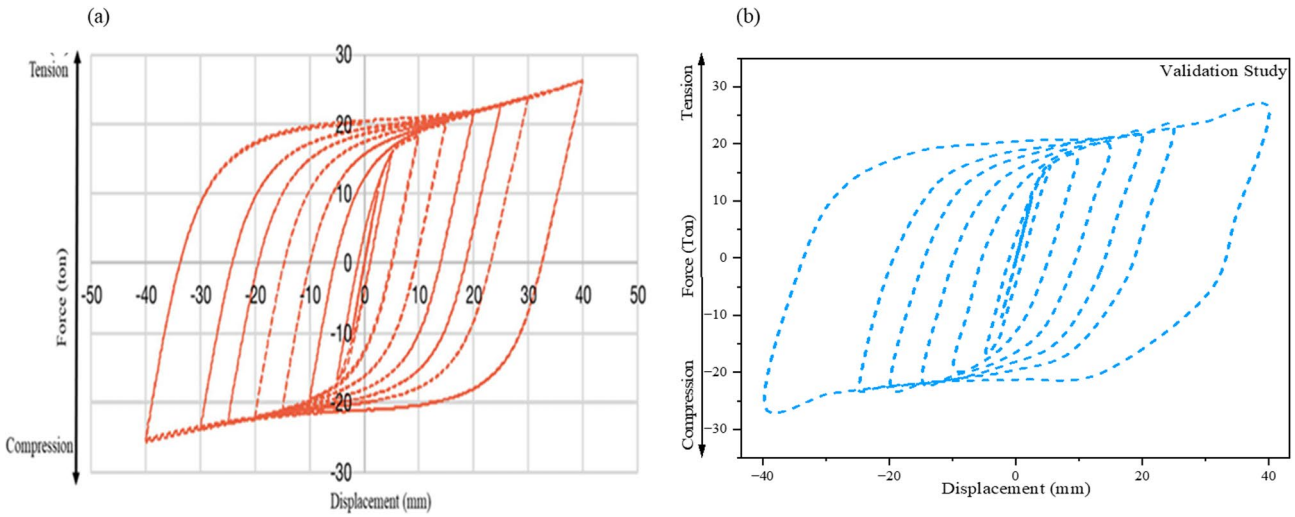

Fig. 4. Force-displacement behaviour of the YBS system, with (**a**) showing experimental results and (**b**) numerical model outcomes.

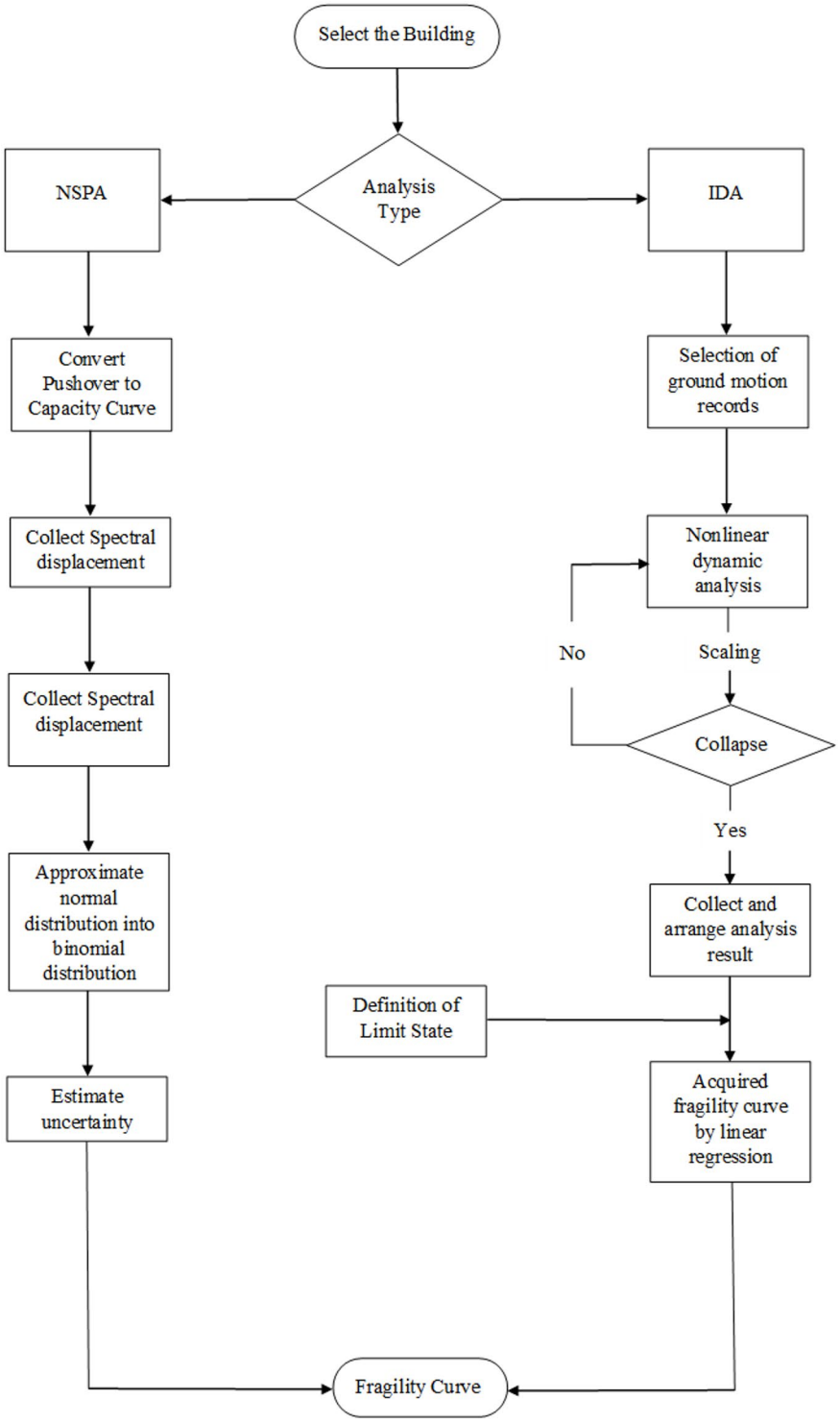

Fig. 5. Methodology adopted for generating seismic fragility curves using nonlinear static and dynamic analysis approaches.

Normalization and scaling of selected ground motions

For reliable seismic performance evaluation, it is essential that the selected ground motions (GMs) represent not only the hazard level of the site but also provide consistent response characteristics with respect to the fundamental period of the structure. Raw earthquake records often show large variability in their peak ground acceleration (PGA), peak ground velocity (PGV), and spectral acceleration shapes, which may not directly correspond to the target design spectrum. To address this, the selected GMs were normalized and scaled so that their median spectral acceleration aligns with the fundamental time period (Ta) of the considered structure. This

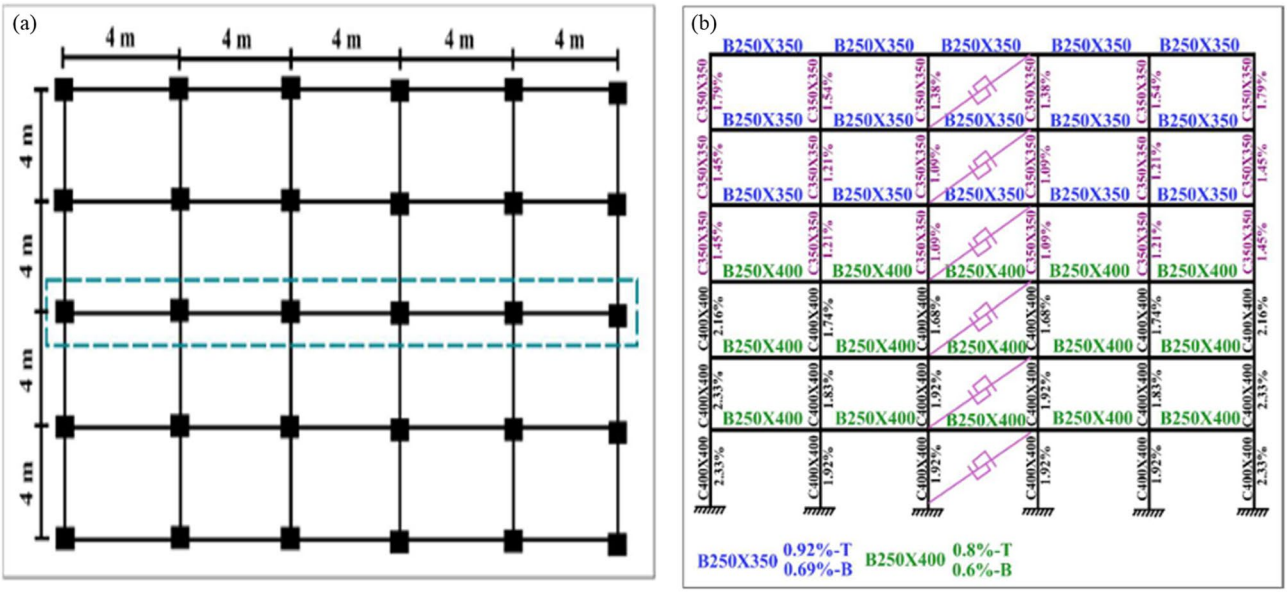

Fig. 6. Six-story, plan-symmetric RC frame: (**a**) plan layout, and (**b**) elevation with member sizes and adopted YBS configuration.

Storey	YBS Connector			HSS section			Total Stiffness and Weight	
	F_d (kN)	K_d (N/mm)	W_d (kN)	Section	W_{hsc} (kN)	K_{hsc} (N/mm)	K_t (N/mm)	W_t (kN)
6	98.1	72373.1	0.3	5(1/2)x5(1/2)x3/16	1.0	93624.1	40815.3	1.3
5	294.2	217119.2	0.5	7×7×1/4	1.7	156043.4	90790.0	2.2
4	490.3	361865.4	1.0	7×7×3/8	2.5	231662.5	141245.2	3.4
3	588.4	434238.5	1.1	7×7×3/8	2.5	231662.5	151071.4	3.6
2	588.4	434238.5	1.1	7×7×3/8	2.5	231662.5	151071.4	3.6
1	686.5	506611.5	1.1	9×9×3/8	3.2	304486.7	190180.4	4.3

Table 1. Finalized YBS properties derived from pushover analysis at 2% target drift for the six-story RC frame.

ensures that the ground motions are compatible with the seismic demand expected for the region and that the structural responses derived from them are realistic. The records were obtained from the PEER-NGA database[32], and the two horizontal components of each motion were examined. For consistency, the larger of the two values of PGA and PGV was considered. Before normalization, PGA values varied between 0.04 g and 0.64 g, with an average of 0.12 g, while PGV ranged from 2.32 cm/s to 36.07 cm/s, averaging 13.83 cm/s. Such variability highlights the need for scaling, as unadjusted motions could either underestimate or overestimate the seismic demand. Normalization factors were applied in the range of 0.38 to 3.82, bringing the records into agreement with the target spectrum at the fundamental period. After normalization, the PGA values reduced to a narrower range of 0.06 g to 0.31 g, with an average of 0.13 g. This adjustment reduced the dispersion in PGA_{max}, thereby providing a more consistent dataset for nonlinear analyses[33–35]. Importantly, normalization did not significantly alter the mean values but made the motions more uniform in terms of intensity.

In addition to PGA and PGV adjustments, the database ensured that ground motions covered a representative spread of seismological and site parameters. The considered events had magnitudes ranging from 6.0 to 7.36, epicentral distances between 13.8 km and 91.15 km, and Vs30 values from 205.78 m/s to 496.46 m/s, covering soft to stiff soil conditions. By selecting motions within these ranges and applying normalization, the dataset captures both variability in source and site conditions while remaining consistent with the design spectrum for Zone V seismicity.

Figure 7(a) shows the individual response spectra of the normalized ground motions compared with the target design spectrum. It highlights that, despite the natural variability of individual records, their collective median closely follows the target across the period range. Figure 7(b) presents the median response spectrum against the target spectrum with a marked fundamental time period of the 6-story building (T_1 = 0.764 s). The close match at this period confirms that the scaling process successfully adjusted the ground motions to be compatible with the structural dynamic properties. Thus, normalization and scaling are necessary steps to ensure that the ground motions not only represent real earthquake records but also conform to the seismic

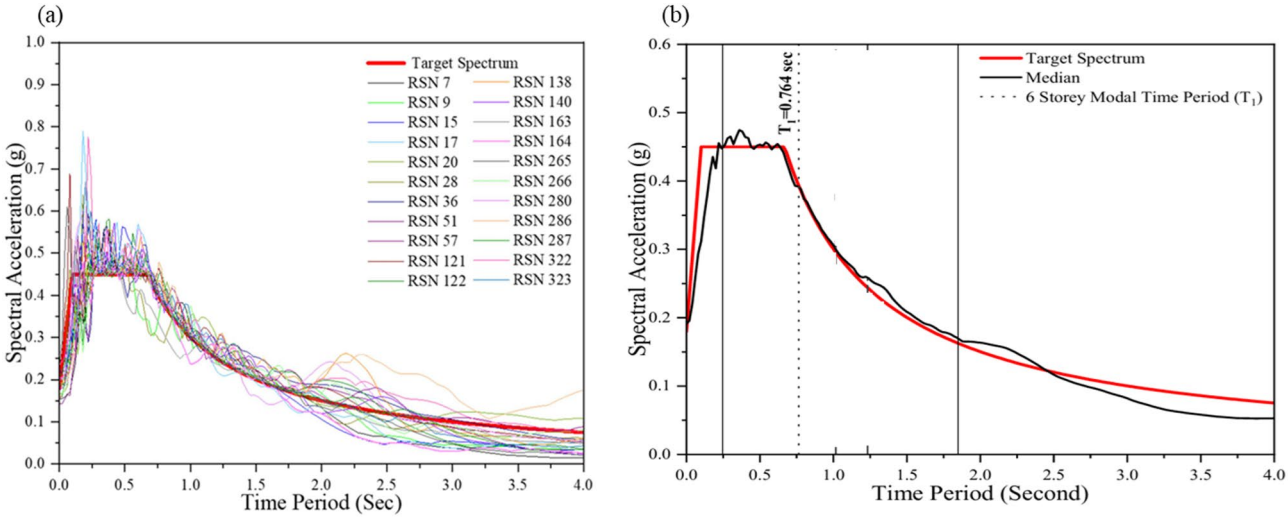

Fig. 7. Ground motion scaling and compatibility: (**a**) normalized response spectra of selected records compared with target spectrum, and (**b**) median spectrum aligned with the fundamental period of the six-story building.

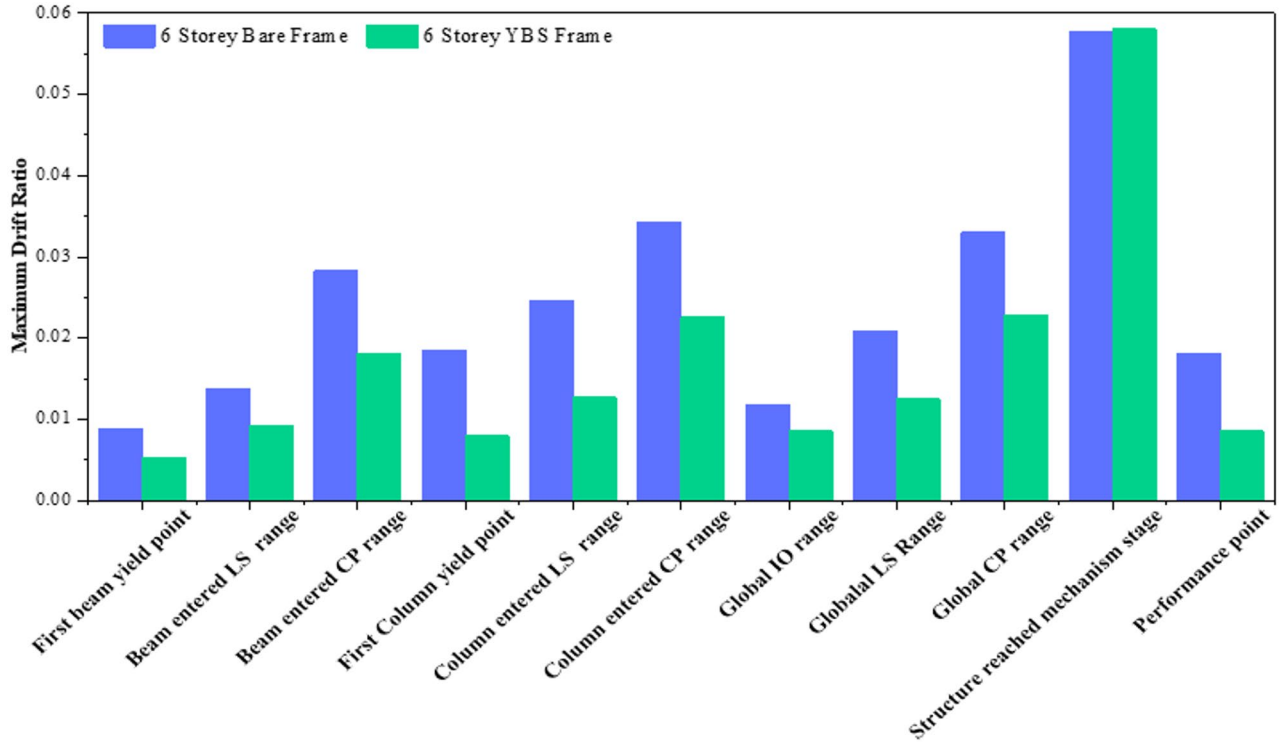

Fig. 8. Comparative maximum drift ratios of six-story bare and YBS-equipped frames showing improved performance and delayed damage progression with YBS incorporation.

design requirements of the study region. This provides a rational basis for assessing structural performance under realistic and code-consistent seismic demands[36,37].

Results and discussion

Damage progression and performance stages

The comparative drift ratio evaluation of the 6-storey bare and YBS-equipped frames shown in Fig. 8 clearly highlights the improved performance achieved through the incorporation of yielding braces. At the first beam yield point, the bare frame exhibited a drift of 0.89% against 0.53% for the YBS frame, a reduction of nearly 40%,

indicating that initial flexural cracks in beams are effectively controlled when additional stiffness is provided. As the structure entered the LS and CP ranges, beams in the YBS frame continued to sustain lower drift levels, with reductions of 32–36% compared to the bare frame, while column yielding was significantly delayed occurring at 0.80% in the YBS frame against 1.85% in the bare frame, almost a 57% improvement. This confirms that all beams undergo cracking and yielding prior to column distress, thereby aligning with the strong-column weak-beam design philosophy. Within the global LS and CP ranges, the YBS system consistently reduced drift demand by 30–40%, and at the performance point the benefit was most evident, where the YBS frame attained a drift of only 0.85% compared to 1.80% for the bare frame, reflecting a reduction of nearly 53%. Up to the 2% drift level, beams experienced progressive flexural cracking, spalling, and eventual yielding, while columns remained largely within the elastic to LS range in the YBS case, whereas the bare frame already exhibited column participation. Overall, the displacement and base shear data from pushover analysis illustrate that the YBS frame provides higher lateral strength, superior drift control, and ensures that inelastic action remains concentrated in beams rather than columns, thereby enhancing seismic safety and delaying the onset of global mechanism formation.

Table 2 and the corresponding pushover curve (Fig. 9) highlight the comparative lateral load behavior of the bare and YBS-equipped frames when expressed in terms of the normalized base shear ratio (V/W). The YBS frame consistently mobilizes higher shear capacity, with V/W reaching up to 0.75 compared to 0.30 in the bare frame, demonstrating enhanced energy dissipation and improved reserve strength. The displacement levels associated with key performance stages also reveal that column yielding is significantly delayed in the YBS frame, ensuring that plasticity remains concentrated in beams until higher load levels are reached. The pushover curve further emphasizes the stiffer initial slope of the YBS system and its ability to maintain higher normalized resistance over a wider displacement range. In terms of deformation capacity, the YBS frame attained a ductility ratio of 3.98, which is superior to the bare frame value of 3.20, confirming its improved ability to undergo larger inelastic deformations without loss of stability. Together, these results validate the superior efficiency of YBS in controlling seismic demands relative to structural weight while also enhancing ductility and collapse safety.

Drift-Based IDA of RC frames

IDA was carried out for the 6-storey RC frame using 22 ground motion records, scaled systematically to cover a PGA range from 0.01 g to 8 g. The scaling was applied in increments of 0.005 g up to 1 g and 0.5 g beyond 1 g, resulting in 36 intensity levels. Nonlinear time history analyses were performed in the X-direction for all records, generating IDA curves expressed in terms of Maximum Inter-storey Drift Ratio (MIDR). Damage thresholds for Immediate Occupancy (IO), Life Safety (LS), and Collapse Prevention (CP) were evaluated following ASCE 41 (2017)[38] guidelines, enabling direct identification of performance ranges at different seismic intensities.

The IDA results for the bare 6-storey frame (Fig. 10a) reveal that drift demands increase rapidly with intensity, and several ground motions exceed the CP threshold at moderate PGA levels, reflecting limited ductility and high dispersion in seismic response. In contrast, the YBS-equipped frame (Fig. 10b) demonstrates significantly improved behaviour: drift demands are consistently lower, IDA curves are more tightly clustered, and the structure remains within IO and LS limits for a wider range of intensities. Only at higher PGA values do some records approach CP, highlighting the ability of YBS to delay collapse mechanisms.

These findings confirm that while the bare frame is vulnerable to severe drift-induced damage, the addition of YBS substantially enhances lateral resistance, reduces seismic demand, and improves collapse safety. The overall improvement is attributed to better energy dissipation and controlled plasticity, validating IDA as an effective tool for performance-based seismic evaluation of mid-rise RC frames.

Stage	Bare Frame			Frame with 2% YBS			Damage State
	Displacement (mm)	Base shear (kN)	W = 1891.63 (kN) V/W	Displacement (mm)	Base shear (kN)	W = 1924 (kN) V/W	
First beam yield point	110	493.6	0.26	120	1134.7	0.59	Slight damage in beam
Beam entered LS range	160	529.7	0.28	180	1265.3	0.66	Moderate damage in beam
Beam entered CP range	320	560.8	0.30	330	1361.7	0.71	Severe damage in beam
First Column yield point	215	555.7	0.29	175	1259.8	0.65	Slight damage in Column
Column entered LS range	280	562.4	0.30	240	1347.0	0.70	Moderate damage in column
Column entered CP range	380	551.0	0.29	405	1423.4	0.74	Severe damage in column
Global IO range	140	514.4	0.27	170	1251.2	0.65	Slight Damage in many beam
Global LS Range	240	559.8	0.30	235	1342.9	0.70	Moderate damage in many beam but slight damage in column
Global CP range	370	552.2	0.29	400	1419.3	0.74	Sevear damage in beams and mderate to slight damge in column
Structure reached mechanism stage.	580	511.0	0.27	620	487.8	0.25	Complete Structure collapsed
Performance point	205	553.48	0.2925	155	1221.56	0.6348	At maximum seismic demand

Table 2. Comparative pushover performance of six-story bare and YBS-equipped RC frames in terms of displacement, base shear ratio (V/W), and damage progression.

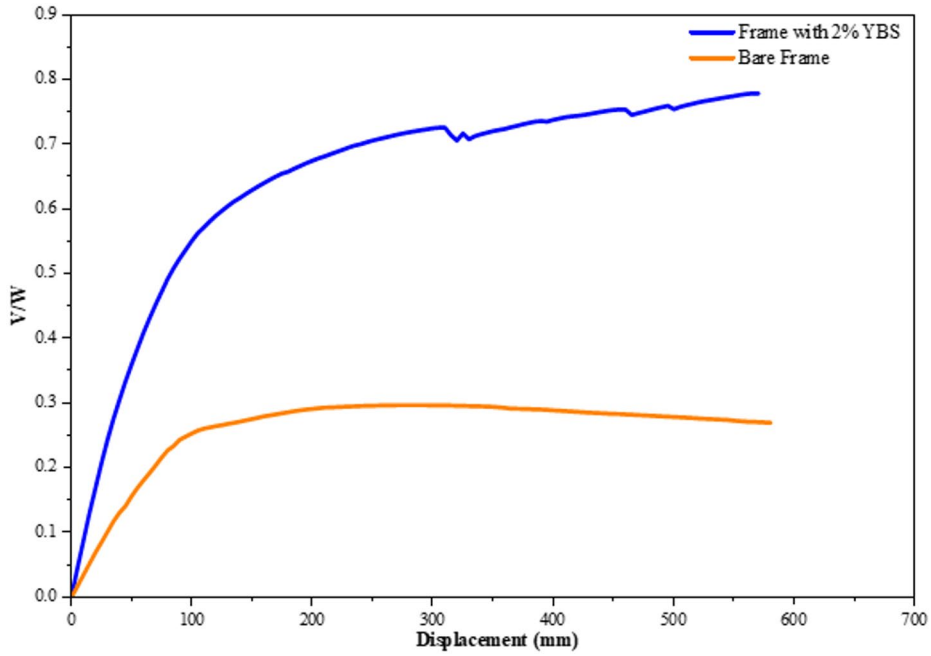

Fig. 9. Pushover curves of six-story bare and YBS-equipped frames showing comparative lateral load behavior in terms of normalized base shear ratio (V/W).

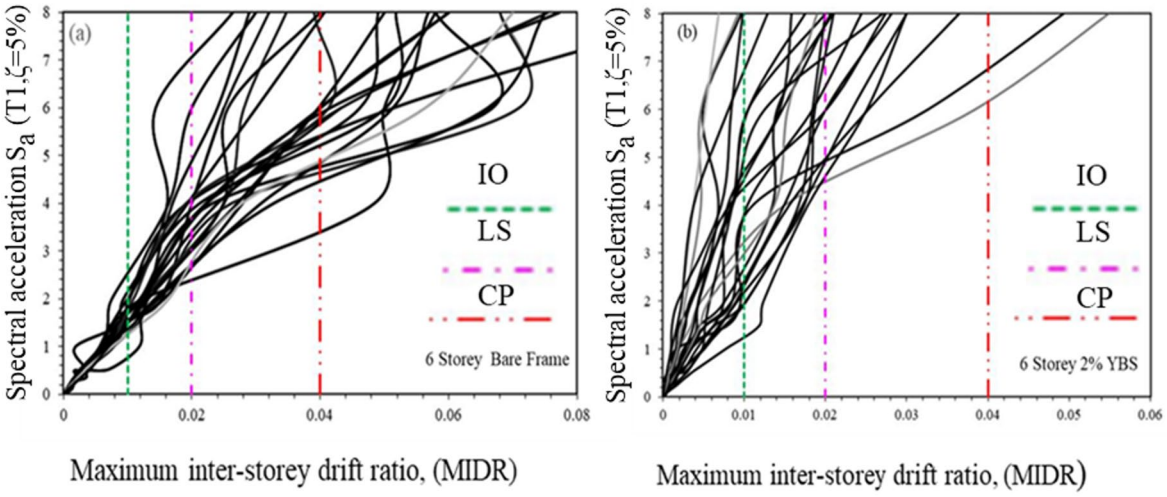

Fig. 10. IDA results of six-story RC frames: (**a**) bare frame and (**b**) YBS frame, showing drift ratios with IO, LS, and CP limits.

The storey drift ratio distribution for the 6-storey building is shown in Fig. 20. The bare frame (Fig. 11a) exhibited larger drift variations, particularly at the middle and upper storeys, with several outliers highlighting its greater vulnerability to excessive lateral displacements. In contrast, the 2% YBS frame (Fig. 11b) demonstrated far more stable performance, with consistently lower drift ratios across all storeys and significantly fewer outliers, confirming its superior capacity to uniformly distribute seismic demands and limit concentration of deformations. A common trend in both systems was higher drift ratios at the lower storeys, where seismic forces accumulate, suggesting that these levels remain critical in overall performance.

The residual drift response of the 6-storey building is presented in Fig. 12. According to FEMA P-58[39] and ASCE 41 (2017)[38], the limiting value for acceptable residual drift is 0.5%. The bare frame exceeded this threshold at several storey levels, indicating a considerable risk of permanent deformation and compromised post-earthquake functionality. Among all the records, the Northern Calif-03 ground motion (RSN 7) at an intensity level of 4 g is specifically highlighted in Fig. 12 to demonstrate the residual drift distribution. This record was chosen because it produced the most severe response among the selected ground motions, even driving the bare

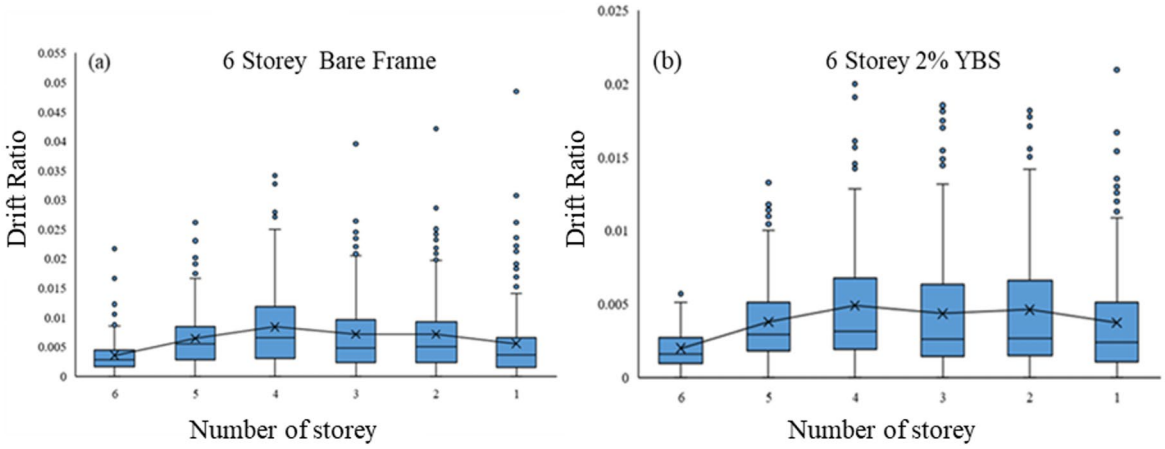

Fig. 11. Storey drift ratio distribution for six-story RC frames: (**a**) bare frame and (**b**) frame with 2% YBS.

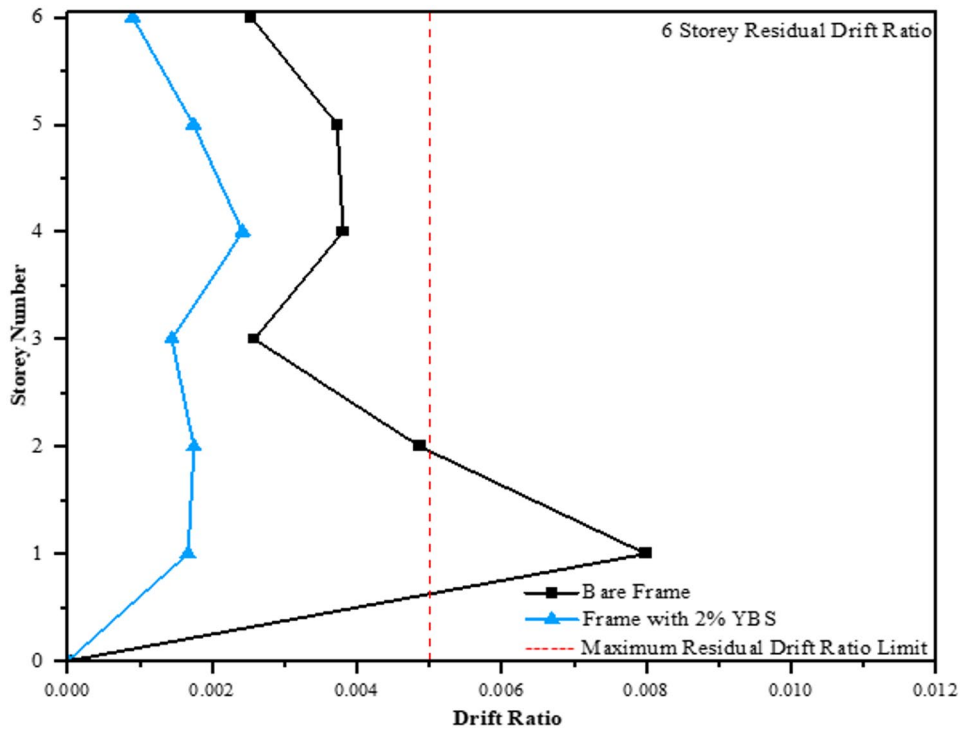

Fig. 12. Residual drift ratio distribution of the six-story RC building under Northern Calif-03 ground motion (RSN 7) scaled to 4 g.

frame to collapse at higher intensity levels, thereby representing a critical scenario for comparison. In contrast, the 2% YBS frame maintained its residual drift ratios well within the 0.5% limit across all storeys, confirming that the system is capable of preventing unacceptable residual displacements. This evaluation highlights that while the bare frame is prone to significant permanent damage, the YBS frame ensures code-compliant performance and improved seismic resilience.

Roof acceleration response of the 6-Storey frame

The roof acceleration time histories of the 6-storey bare frame and the 6-storey frame equipped with 2% YBS are illustrated in Fig. (13a) and Fig. (13b), respectively. Roof acceleration is a critical response parameter as it directly reflects the amplification of ground motion at the top of the structure, influencing both occupant safety and the vulnerability of non-structural components. Excessive roof accelerations can induce significant secondary damage, even if the primary structural system remains intact.

For the bare frame (Fig. 13a), roof acceleration peaks reached values exceeding 30 m/s² under the Northern Calif-03 ground motion (RSN 7) at 4 g intensity, indicating strong amplification effects and substantial inertial

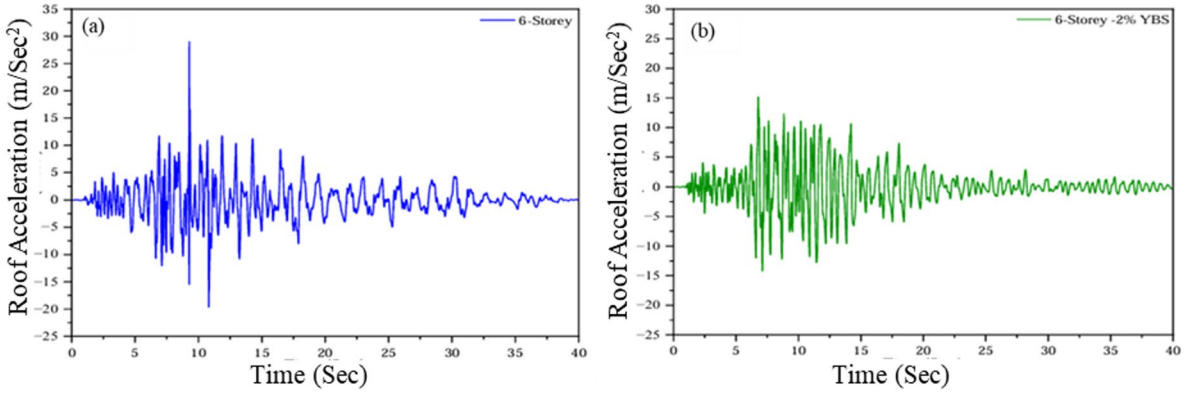

Fig. 13. Roof acceleration time histories of the six-story RC building: (**a**) bare frame and (**b**) frame with 2% YBS, under Northern Calif-03 ground motion (RSN 7) scaled to 4 g.

Storey no	Inter-story drift ratio			Floor acceleration (g)			Residual inter-story drift ratio		
	Bare Frame	YBS Frame	Reduction (%)	Bare Frame	YBS Frame	Reduction (%)	Bare Frame	YBS Frame	Reduction (%)
6	0.0032	0.002	37.5	0.55	0.29	47.3	0.00254	0.000904	64.4
5	0.0068	0.0036	47.1	0.50	0.26	48.0	0.00373	0.00174	53.3
4	0.01	0.0039	61	0.44	0.19	56.8	0.00381	0.00242	36.5
3	0.0071	0.0034	52.1	0.38	0.17	55.3	0.00254	0.00144	43.3
2	0.01	0.0036	64.0	0.33	0.13	60.6	0.00487	0.00175	64.1
1	0.008	0.0023	71.3	0.28	0.1	64.3	0.008	0.00167	79.1

Table 3. Comparison of Inter-Story drift Ratio, floor Acceleration, and residual drift reduction in bare and YBS frames at each storey Level.

demands on the structure. In contrast, the YBS-equipped frame (Fig. 13.b) demonstrated much lower peak roof accelerations, with amplitudes reduced by nearly one-third and a visibly smoother response profile. The reduction in acceleration is attributed to the added energy dissipation and enhanced stiffness provided by the yielding braces, which limit the transfer of seismic energy to the upper storeys.

Table 3 presents a comparative evaluation of the seismic response parameters for the bare and Yielding Base Shear (YBS) frames. The inter-story drift ratio and floor acceleration values represent the mean response averaged over all considered ground motions, reflecting the overall improvement in global deformation and inertial response due to the YBS system. Conversely, the residual inter-story drift ratio values correspond specifically to the Northern California–03 (RSN 7) ground motion at an input intensity of 4 g, highlighting the post-yield deformation control capacity of the YBS frame under severe excitation. As observed, the YBS frame demonstrates a consistent reduction across all parameters, with drift, acceleration, and residual drift reduced by approximately 37–71%, 47–64%, and 36–79%, respectively, indicating its superior energy dissipation and self-centering performance compared to the conventional bare frame.

Hysteretic response and energy dissipation of the 6-Storey YBS frame

The hysteretic response of the 6-storey RC frame equipped with a 2% YBS configuration was examined under the Northern Calif-03 ground motion (RSN 7) at 4 g intensity, chosen due to its significant damage potential observed in the bare frame case. Figure 14 illustrates the hysteresis loops for each storey, providing insight into the force–deformation characteristics and energy dissipation capacity of the system. The results indicate that the YBS elements developed forces exceeding their nominal design strength, revealing an inherent over strength capacity that contributes to improved seismic resilience. Distinct and stable hysteresis loops were observed across all storeys, with wide loops at the lower storeys (1st to 3rd) showing higher force and deformation demand, and gradually narrower loops at the upper storeys (4th to 6th), consistent with reduced seismic demand at higher levels. Importantly, the YBS exhibited stable cyclic behaviour with negligible strength or stiffness degradation, and returned close to its original position after unloading, confirming the absence of significant residual deformation.

This behaviour highlights the system's ability to dissipate seismic energy efficiently through repeated loading cycles, thereby limiting permanent structural damage. The progressive reduction in loop width from lower to upper floors indicates that seismic energy is absorbed more effectively at the base, reducing drift concentrations at critical levels. These findings validate that the 2% YBS configuration not only improves overall structural

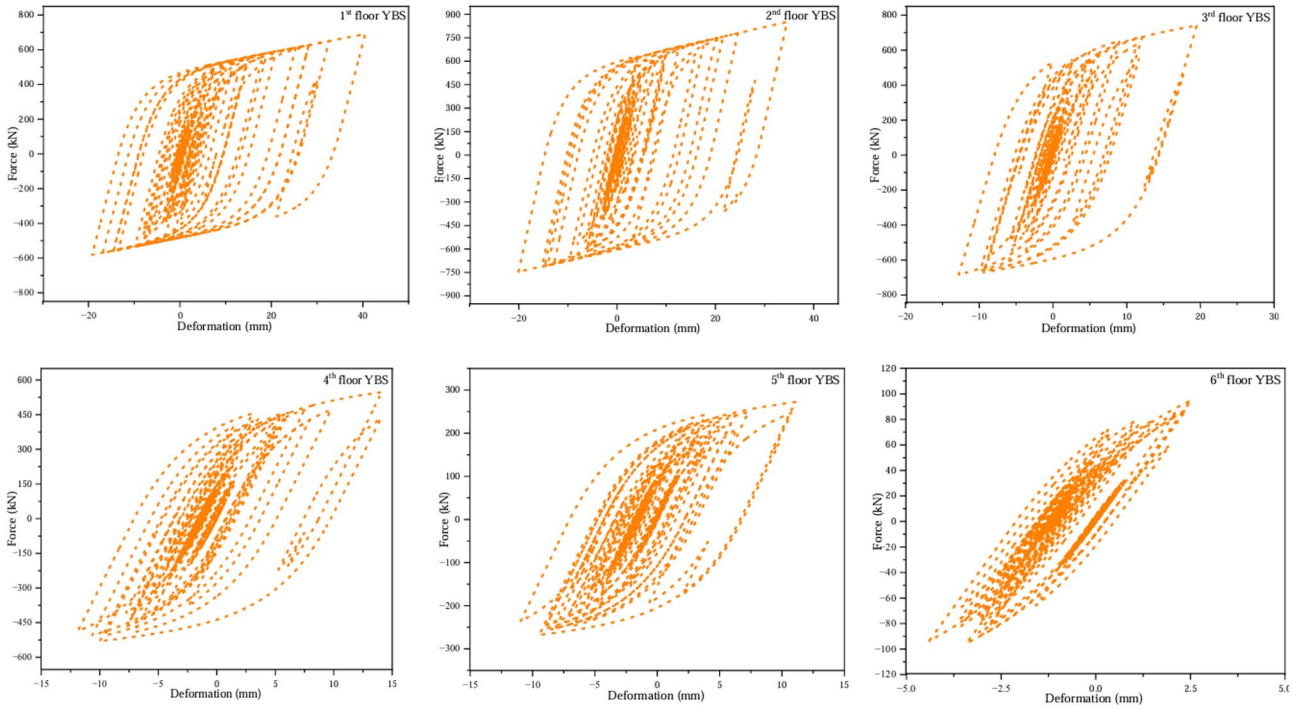

Fig. 14. Storey-wise hysteresis loops of the six-story RC frame with 2% YBS under Northern Calif-03 ground motion (RSN 7) at 4 g intensity.

durability during high-intensity shaking but also ensures a favourable distribution of seismic forces along the building height. While similar patterns were observed in other configurations, the 6-storey results are presented as representative, demonstrating the reliability of YBS in enhancing seismic performance of mid-rise RC buildings.

Probabilistic seismic vulnerability assessment of 6-Storey bare and YBS frames

Seismic fragility analysis provides a probabilistic framework to quantify the likelihood of RC frames exceeding predefined damage thresholds under varying earthquake intensities. Performance levels IO, LS, and CP were defined using inter-storey drift ratios and spectral displacement thresholds, with the capacity spectrum curve subdivided into slight, moderate, severe, and complete damage states according to Eq. (1). The IDA approach further incorporated drift thresholds of 1%, 2%, and 4% in line with FEMA P-695[38] and recent literature[22,25,34]. Fragility functions were expressed through a lognormal distribution as given in Eq. (2), where μ_k represents the median seismic demand at which a given damage state is reached and β_k accounts for variability and uncertainty in structural response, with higher β values reflecting greater dispersion. The resulting fragility curves were calibrated using statistical fitting to capture these uncertainties. In this study, pushover-based seismic fragility analysis was adopted, wherein the capacity curve obtained from nonlinear pushover analysis was combined with seismic demand models to estimate the probability of reaching or exceeding different damage states. Using spectral displacement (S_d) as the intensity measure, the fragility functions were derived through both binomial and normal cumulative distribution models, as illustrated in Fig. 15. The curves show the exceedance probability for slight, moderate, severe, and complete damage states, where the steeper slopes represent higher sensitivity of the frame to seismic demand. The comparison between binomial and normal fits highlights the robustness of the derived fragility functions in capturing uncertainty across damage states.

Findings for the 6-storey bare frame (Table 4) revealed a nearly uniform probability of exceedance across all damage states, signifying significant vulnerability and a high likelihood of collapse even at lower intensity measures. By contrast, the introduction of YBS elements enhanced resilience: a 1% YBS configuration reduced the collapse probability, while a 2% YBS configuration provided the most pronounced improvement, substantially lowering collapse risk and enhancing the system's energy dissipation capacity. The fragility curves for the 6-storey frames (Figs. 15 and 16) clearly demonstrated reduced seismic risk in the YBS-integrated systems compared with the bare frame. Moreover, IDA results exhibited strong linear correlations between seismic demand and structural response across damage states, validating the consistency of behavior and confirming that YBS configurations significantly improve seismic performance in mid-rise RC buildings[22,39].

$$S_{d,k} = \begin{cases} S_{d1} = 0.7D_y & slight\ damage\ state \\ S_{d2} = D_y & moderate\ damage\ state \\ S_{d3} = D_y + 0.25\ (D_u - D_y) & severe\ damage\ state \\ S_{d4} = D_u & complete\ damage\ state \end{cases} \quad (1)$$

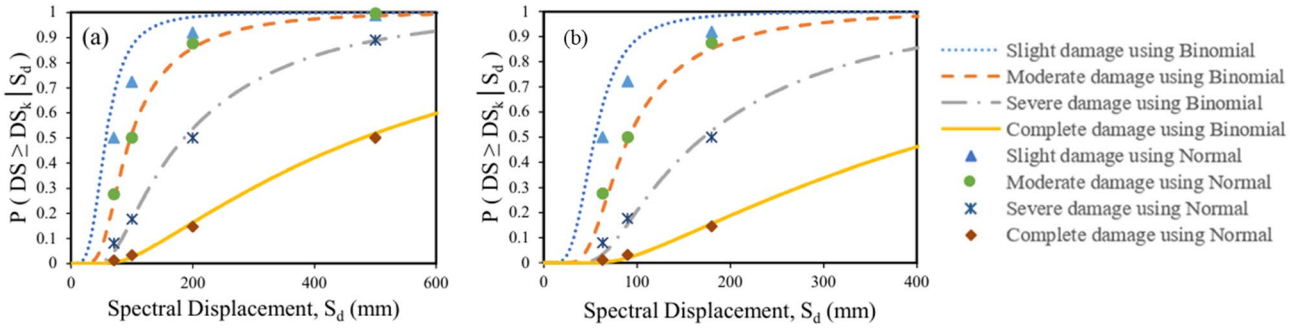

Fig. 15. Pushover-based seismic fragility analysis of the selected 6-storey RC frame building: (**a**) bare frame; (**b**) frame with 2% YBS.

Damage State	Fixing Condition	d	Ds1	DS2	DS3	DS4
Slight	SD_1	0.229	0.500	0.283	0.073	0.013
Moderate	SD_2	0.377	0.717	0.500	0.166	0.034
Severe	SD_3	0.631	0.927	0.877	0.500	0.151
Complete	SD_4	0.858	0.987	0.996	0.895	0.500

Table 4. Shows that the exceedance probabilities across all damage States for the 6-storey bare frame are nearly uniform, with each state exhibiting about 50% likelihood.

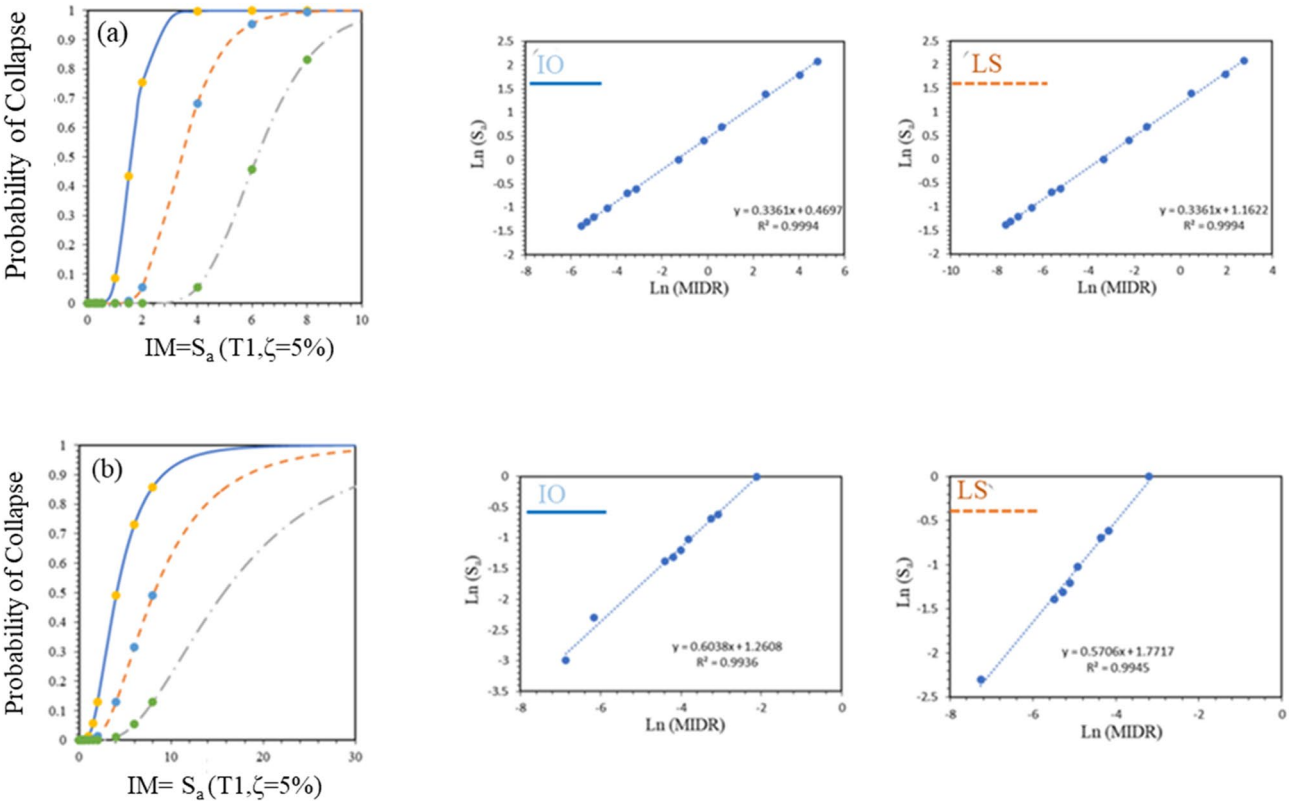

Fig. 16. Collapse probability versus intensity measure IM = S_a (T1, ζ = 5%) and corresponding fragility functions derived from traditional IDA for the 6-storey RC frame: (**a**) bare frame; (**b**) frame with 2% YBS.

Model	Spectral Displacement (mm)		IM (Spectral Acceleration) (m/s²)	
	10%	50%	10%	50%
6-Storey Bare Frame	160	446	3.6	5.1
6-Storey with 2% YBS	173	460	8	15

Table 5. Presents a comparison of the probability of exceedance at 10% and 50% for complete damage States of the selected RC frame buildings, as obtained from NSPA and IDA.

$$P\left[DS \geq DS_k ?\mathrm{X} = \Theta\right] = \varnothing\left[\frac{1}{\beta_k}\ln\left(\frac{\Theta}{\mu_k}\right)\right] \tag{2}$$

Table 5 presents the spectral displacement and spectral acceleration values corresponding to 10% and 50% probability of exceedance for the complete damage state in the 6-storey RC frames. For the bare frame, the spectral displacement was 160 mm and 446 mm at 10% and 50% probability levels, with corresponding intensity measures of 3.6 m/s² and 5.1 m/s², respectively. In contrast, the 6-storey frame with 2% YBS showed slightly higher spectral displacement values of 173 mm and 460 mm, but required much larger seismic intensities of 8 m/s² and 15 m/s² to reach the same exceedance probabilities. This clearly indicates that although lateral displacement demand increases marginally with YBS, the system significantly enhances strength and energy absorption, thereby reducing collapse risk under higher seismic loads. The fragility curves for the 6-storey frames further validate this outcome, highlighting a marked reduction in the probability of severe and complete damage in the YBS-integrated case compared with the bare frame, confirming the effectiveness of YBS in improving seismic resilience.

Conclusion

This study presented a comprehensive seismic performance assessment of a six-storey RC frame with and without the integration of a YBS. A multi-analysis framework incorporating NSPA, NLTHA, IDA and probabilistic fragility evaluation was employed to capture global capacity, dynamic response, and collapse vulnerability, Key findings are as follows:

- Enhanced drift and strength performance: The YBS-equipped frame consistently limited inter-storey drift demands by 30–53% compared with the bare frame, while simultaneously mobilizing higher normalized base shear ratios (up to 0.75 versus 0.30), confirming superior lateral load resistance and compliance with the strong-column weak-beam design philosophy.
- Improved ductility and energy dissipation: The ductility ratio of the YBS frame (3.98) exceeded that of the bare frame (3.20), and storey-wise hysteresis loops demonstrated stable cyclic energy dissipation with negligible degradation, highlighting the capacity of YBS to absorb seismic input energy without inducing residual deformations.
- Dynamic performance gains: Incremental dynamic analysis revealed that the bare frame rapidly exceeded Collapse Prevention thresholds under moderate shaking, whereas the YBS frame-maintained performance within Immediate Occupancy and Life Safety limits across a wider range of ground motion intensities. Residual drift responses in the YBS frame consistently remained below the 0.5% threshold recommended by FEMA P-58 and ASCE 41, ensuring functional recovery after earthquakes.
- Probabilistic risk reduction: Fragility analyses established that the bare frame exhibited nearly uniform exceedance probabilities (~ 50%) across all damage states, whereas YBS incorporation substantially shifted collapse probabilities to higher intensity measures. For the complete damage state, the bare frame reached 50% exceedance at 5.1 m/s², while the YBS frame required 15 m/s², reflecting a threefold enhancement in collapse safety margin.
- Collectively, these results demonstrate that YBS integration significantly improves the seismic resilience of mid-rise RC buildings by reducing drift concentration, delaying column yielding, limiting residual deformations, and lowering collapse risk. Beyond structural efficiency, YBS offers a practical and economical solution for both retrofitting existing vulnerable frames and designing new constructions in high seismic zones, particularly in densely populated urban regions where soft-storey mechanisms remain critical.

In a broader societal context, this work contributes to the United Nations Sustainable Development Goals (SDGs) by advancing resilient infrastructure (SDG 9), supporting sustainable cities and communities (SDG 11), and reinforcing climate action through disaster risk reduction (SDG 13). By demonstrating the effectiveness of YBS in improving structural safety and functionality under seismic events, the study directly supports global efforts toward sustainable, disaster-resilient urban development.

While the study confirms the effectiveness of YBS through detailed numerical simulations, future work should focus on large-scale experimental validation, life-cycle cost analysis, and exploration of hybrid systems that combine YBS with supplementary damping or isolation technologies. Such efforts will further establish YBS as a reliable component of performance-based seismic design frameworks and support its integration into national and international seismic codes.

Data availability

The datasets generated during and/or analyzed during the current study are available from the corresponding author on reasonable request.

Received: 7 September 2025; Accepted: 29 October 2025
Published online: 27 November 2025

References

1. Aggarwal, Y., Baddipalli, S. & Saha, S. K. Construction practices and seismic vulnerability of buildings in the Indian Himalayan region: A case study. *Nat. Hazards Rev.* **25** (2), 05024002. https://doi.org/10.1061/NHREFO.NHENG-1902 (2024).
2. Earthquake zones. of India - Wikipedia.
3. Jain, S. K. Earthquake safety in india: achievements, challenges and opportunities. *Bull. Earthq. Eng.* **14** (5), 1337–1436. https://doi.org/10.1007/s10518-016-9870-2 (2016).
4. Ansari, A. et al. Fuzzy synthetic approach for seismic risk assessment of bridges with insights from the 2023 Kahramanmaras earthquake in Turkiye. *Sci. Rep.* **15** (1), 13418. https://doi.org/10.1038/s41598-025-98277-5 (2025).
5. Jena, R. et al. Earthquake vulnerability assessment for the Indian Subcontinent using the long Short-Term memory model (LSTM). *Int. J. Disaster Risk Reduct.* **66**, 102642. https://doi.org/10.1016/j.ijdrr.2021.102642 (2021).
6. https://www.globalquakemodel.org/product/openquake-engine
7. BIS (Bureau of Indian Standards). *Criteria for Earthquake Resistant Design of Structures: Part 1. General Provisions and buildings. IS 1893* (BIS, 2016a).
8. BIS (Bureau of Indian Standards). *Criteria for Earthquake Resistant Design of Structures: Part 1. General Provisions and buildings. IS 1893* (BIS, 2023).
9. Leblouba, M. Selection of seismic isolation system parameters for the near-optimal design of structures. *Sci. Rep.* **12** (1), 14734. https://doi.org/10.1038/s41598-022-19114-7 (2022).
10. ASCE/SEI (ASCE/Structural Engineering Institute). Minimum design loads for buildings and other structures. ASCE/SEI 7–16, Reston, VA. (2016).
11. Bhasker, R. & Menon, A. Towards an appropriate seismic vulnerability assessment model in India. In *16th world conference on earthquake engineering*. (2017).
12. Zhou, Y., Lie, W., Zhang, Q., Hong, J. & Li, D. Development and experimental study of a novel rotational metallic damper. *Eng. Struct.* **315**, 118453 (2024).
13. Lie, W., Zhou, Y., Zhang, Q. & Hong, J. Development of a novel rotational metallic damper as a dissipative connector in rocking steel core systems: Cyclic behavior and seismic demand. *J. Building Eng.* **98**, 111237 (2024).
14. Lie, W., Zhou, Y., Zhang, Q., Hong, J. & Chen, Z. Potential use of rotational metallic dampers for seismic enhancement of infilled RC frames with open first story. *Eng. Struct.* **322**, 119080 (2025).
15. Beiraghi, H. Seismic response of dual structures comprised by Buckling-Restrained braces (BRB) and RC walls. *Struct. Eng. Mechanics: Int. J.* **72** (4), 443–454 (2019).
16. Beiraghi, H. & Zhou, H. Dual-steel frame consisting of moment-resisting frame and shape memory alloy braces subjected to near-field earthquakes. *Struct. Des. Tall Special Build.* **29** (14), e1784 (2020).
17. Beiraghi, H. Seismic response of buckling restrained braced frame with strong back system. *INGEGNERIA SISMICA*. **37** (4), 65–82 (2020).
18. Bobadilla, H. G. et al. Cumulative ductility and fatigue life of Buckling-Restrained braces under severe seismic loading conditions: an experimental study. *Soil Dyn. Earthq. Eng.* **199**, 109700 (2025).
19. Hoveidae, N. Ultra-low cycle fatigue fracture life of a type of buckling restrained Brace. *J. Rehabilitation Civil Eng.* **6** (2), 29–42 (2018).
20. Gray, M. G., Christopoulos, C. & Packer, J. A. Cast steel yielding Brace system for concentrically Braced frames: concept development and experimental validations. *J. Struct. Eng.* **140** (4), 04013095. https://doi.org/10.1061/(ASCE)ST.1943-541X.0000910 (2014).
21. Información Técnica. DAMPO. https://www.dampo.com.mx/informacion-tecnica (2021).
22. Rc, B., Shirkol, A. I., Gondaliya, K. & Biradar, B. B. Seismic performance and fragility assessment of RC frame buildings equipped with yielding Brace systems using NSPA and IDA. *J. Struct. Des. Constr. Pract.* **30** (4), 04025065. https://doi.org/10.1061/JSDCCC.SCENG-1726 (2025).
23. ETABS: Building Analysis and Design, Computers & Structures, I. (n.d.). https://www.csiamerica.com/products/etabs
24. Charalampakis, A. E. & Koumousis, V. K. On the response and dissipated energy of Bouc–Wen hysteretic model. *J. Sound Vib.* **309** (3–5), 887–895. https://doi.org/10.1016/j.jsv.2007.07.080 (2008).
25. Vyas, R., Rc, B., Gondaliya, K. & Shirkol, A. I. Seismic fragility assessment and comparative study of modified performance based plastic design method for reinforced concrete frames. https://doi.org/10.1061/JSDCCC/SCENG-2087 (2025).
26. Mander, J. B., Priestley, M. J. & Park, R. Theoretical stress-strain model for confined concrete. *J. Struct. Eng.* **114** (8), 1804–1826. https://doi.org/10.1061/(ASCE)0733-9445(1988)114:8(1804) (1988).
27. Priestley, M. N., Seible, F. & Calvi, G. M. *Seismic Design and Retrofit of Bridges* (Wiley, 1996).
28. BIS (Bureau of Indian Standards). Design loads (Other than Earthquake) for buildings and structures. Dead loads—Code of practice. IS 875 Part 1. New Delhi, India: BIS. (1987a).
29. BIS (Bureau of Indian Standards). Design loads (Other than Earthquake) for buildings and structures. Imposed loads—Code of practice. IS 875 Part 2. New Delhi, India: BIS. (1987b).
30. BIS (Bureau of Indian Standards). *Ductile detailing of reinforced concrete—Code of practice. IS 13920*. (New Delhi, India, BIS, 2016b).
31. BIS (Bureau of Indian Standards). *Plain and Reinforced concrete— Code of practice. IS 456* (BIS, 2000).
32. *PEER Ground Motion Database - PEER Center*. (n.d.) https://ngawest2.berkeley.edu (**Accessed March 2025**).
33. Vyas, R., Rc, B., Ansari, A., Gondaliya, K. & Shirkol, A. I. Seismic performance assessment of RC buildings under Turkey ground motions designed by force based design and improved performance based plastic design method. *Asian J. Civil Eng.* **26** (3), 1355–1371. https://doi.org/10.1007/s42107-024-01255-x (2025).
34. Gondaliya, K., Amin, J., Bhaiya, V., Vasanwala, S. & Desai, A. Generating seismic fragility curves of RC frame Building using NSPA and IDA. *Asian J. Civil Eng.* **24** (2), 523–538. https://doi.org/10.1007/s42107-022-00516-x (2023).
35. Palsanawala, T. N., Vasanwala, S. A., Bhaiya, V. & Gondaliya, K. M. Seismic fragility of RC wall-frame buildings using the DDBD approach for vulnerability assessment. *Pract. Periodical Struct. Des. Constr.* **28** (4), 04023056. https://doi.org/10.1061/PPSCFX.SCENG-1286 (2023).
36. FEMA. Quantification of Building seismic performance factors. FEMA P695. Washington, DC: FEMA. (2009).
37. FEMA. *Seismic Performance Assessment of buildings. FEMA P-58* (FEMA, 2018).
38. ASCE. *Seismic Evaluation and Retrofit of Existing Buildings* (ASCE/ SEI 41 – 17, 2017).
39. Barbat, A. H., Pujades, L. G. & Lantada, N. Seismic damage evaluation in urban areas using the capacity spectrum method: application to Barcelona. *Soil Dyn. Earthq. Eng.* **28**, 10–11. https://doi.org/10.1016/j.soildyn.2007.10.006 (2008).

Acknowledgements
"The authors extend their appreciation to Northern Border University, Saudi Arabia, for supporting this work through project number (NBU-CRP-2025-2461).

Author contributions
"B.R. V.R. A.I.S. A.A. R.V. K.G. and P.D.: Main author, conceptualization, literature review, manuscript preparation, application of fuzzy models, methodological development, statistical analysis, detailing, and overall analysis; Y.F. A.E.A. N.R.C. R.G. and P.M.: Data compilation, data analysis, comprehensive analysis, detailed review, and editing".

Funding
The first author gratefully acknowledges the Ministry of Education, Government of India, for providing the scholarship support for pursuing the Ph.D. program. This research was supported and funded by the Internal Grants - Sultan Qaboos University Research Funds with reference number IG/–/DVC/EMC/25/121. For the same project, the previous reference was IG/DVC/EMC/25/01.

Declarations

Competing interests
The authors declare no competing interests.

Additional information
Correspondence and requests for materials should be addressed to B.R., A.I.S., N.R.C., R.G. or A.A.